Transactions of the **14th International Conference on Structural Mechanics in Reactor Technology** (SMiRT 14), Lyon, France, August 17-22, 1997

L02/3

Inelastic behavior of Mod. 9Cr-1Mo steel and its description by constitutive model considering dynamic strain aging

Yaguchi M., Takahashi Y.
Central Research Institute of Electric Power Industry, Japan

ABSTRACT
A series of deformation tests has been conducted with Mod.9Cr-1Mo steel. Interesting behavior which was hardly described by conventional constitutive models was observed. In order to describe the behavior adequately, a unified constitutive model incorporating dynamic strain aging was proposed. Simulations by the model agreed with experimental results very well.

1. INTRODUCTION

Modified 9Cr-1Mo steel was developed at ORNL as a structural material and is a principal candidate material for a steam generator component of Demonstration Fast Breeder Reactor (DFBR) in Japan(1). Since an inelastic analysis plays a very important role in structural design of DFBR, a development of an accurate inelastic constitutive model and its application to FEM programs are strongly needed(2).

As a first stage of developing the constitutive model, the authors have conducted a series of deformation tests with Mod.9Cr-1Mo steel at various temperatures. It was found out that this material shows interesting behavior which cannot be described even qualitatively by conventional unified constitutive models. Therefore, the authors proposed a unified model considering dynamic strain aging effect in order to describe the inelastic behavior precisely. The validity of the model was discussed with simulations for various loading conditions.

2. INELASTIC BEHAVIOR OF MODIFIED 9Cr-1Mo STEEL

2.1 Test procedure

Test material was hot rolled Mod.9Cr-1Mo steel and was subjected to heat treatment of normalizing[1060°C x 90min] and tempering [760°C x 60min], followed by a heat treatment corresponding to post-weld heat treatment[PWHT; 740°C x 504min]. Table 1 and 2 give a chemical composition of the material and mechanical properties at R.T., respectively. Test specimens were standard type one[Gauge Length:10mm, Diameter:10mm] and were machined from the plate in the rolling direction.

A test facility was an electro-mechanical driven type fatigue testing machine with an induction heating device. Measurement of strain was made by a quartz rod contact type high temperature extensometer.

All tests were carried out under total strain control in air at 200°C, 400°C, 500°C, 550°C and

600°C. Imposed strain type was a monotonic tension and strain hold waveform, as shown in Fig.1. Strain rates for loading portion were in the range of between $10^{-6}s^{-1}$ and $10^{-3}s^{-1}$. When strain reached the point of 1.5%, the strain waveform changed from the ramp type to the hold type. Duration of the strain hold was up to 24hr for all conditions.

2.2 Test results

Figure 2 summarizes the test results by showing relationships between peakstress, stress at hold end and the temperatures. The relationships between the peakstress and the temperature for each strain rate were expressed by bilinear curve of Arrhenius type Eq.(1), and time/rate dependency was different above 500°C and below 400°C.

$$\sigma_{peak} = M_1 \exp(\frac{M_2}{T_{abs}}) \qquad (1)$$

where σ_{peak} is peakstress, T_{abs} is absolute temperature and M_1, M_2 is material constants(Table 3). The inelastic behavior for each temperature region was as follows.

1) Above 500°C

When the temperature was above 500°C, this material showed rate dependency of a monotonic stress-strain curve and stress relaxation behavior, as shown in Fig.3 and Fig.4, respectively. A degree of the rate dependency and the stress relaxation become larger with increasing of the test temperature.

In Fig.4, very interesting behavior was observed. While an initial stress for the hold period showed higher value as the prior loading strain rate was higher, a stress after the relaxation showed opposite tendency; that is, the relaxed stress showed higher value when the prior strain rate was lower(3). This behavior cannot be expressed even qualitatively by conventional existing unified constitutive models.

2) Below 400°C

When the temperature was below 400°C, the monotonic curve did not show rate dependency, however large stress relaxation was observed, as shown in Fig.5 and Fig.6, respectively. This behavior was also quite unique, for this means that the time/rate dependency depends on the loading conditions. This behavior is hardly described by conventional unified models, too. The dependency of the relaxed stress on the prior loading strain rate was also observed for this temperature region.

Analyzing the test results carefully, the authors thought that the strange behavior was due to the dynamic strain aging effect which is caused by moving solute atoms and sometimes brings about negative strain rate dependency(4). A modeling of the aging effect was tried in the next section.

3. UNIFIED CONSTITUTIVE MODEL INCORPORATING DYNAMIC STRAIN AGING EFFECT

3.1 Basic concept

In order to describe the inelastic behavior of Mod.9Cr-1Mo steel adequately, the authors proposed a unified constitutive model considering the dynamic strain aging effect. In this model, an applied stress consists of three stress components; a backstress, an overstress and an aging stress which shows the negative strain rate dependency.

Figures 7 and 8 show schematic illustrations of the model below 400°C. In Fig.7, it was supposed for simplicity that the aging stress exists for slow straining only and static recovery of the backstress is negligible. In this model, the rate independence of the monotonic curve was explained as the difference between the overstress for the fast straining and that for the slow straining is just equal to the aging stress for the slow straining. When the strain hold period starts, the overstress decreases with the hold time and the stress relaxation occurs. As for the relaxed stress dependency on the prior loading strain rate as shown in Fig.8, it was explained that the relaxed stress for the prior slow straining shows higher value than that for the prior fast straining due to the aging stress developed during the prior slow straining period.

Generally, the model could describe both the positive and the negative rate dependency and much complex behavior, because there is the static recovery of the backstress and the rate dependency of the aging stress does not always correspond to that of the overstress.

3.2 Formulation

The model is expressed in a uniaxial form as follows.

$$\dot{\varepsilon}_{in} = \left\langle \frac{|\sigma - X| - \sigma_a}{D} \right\rangle^n sgn(\sigma - X) \qquad (2)$$

$$\dot{X} = C\left(a\dot{\varepsilon}_{in} - X\left|\dot{\varepsilon}_{in}\right|\right) - \gamma |X|^m sgn(X) \qquad (3)$$

$$\dot{\sigma}_a = b(\sigma_{as} - \sigma_a)\left|\dot{\varepsilon}_{in}\right| \qquad (4)$$

$$b = b_1 \text{ for } \sigma_{as} - \sigma_a < 0 \qquad (5)$$

$$b = b_2 \text{ for } \sigma_{as} - \sigma_a \geq 0 \qquad (6)$$

$$\sigma_{as} = A + B\log_{10}\left|\dot{\varepsilon}_{in}\right|,\ \sigma_{as} \geq 0 \qquad (7)$$

where, X represents the backstress, σ_a represents the aging stress, whose asymptotic value is denoted by σ_{as}, $D, n, C, a, \gamma, m, b_1, b_2, A$ and B are material constants. The bracket $< >$ indicates that $<x> = 0$ if $x < 0$ and $<x> = x$ if $x \geq 0$.

The model was proposed referring to the Chaboche model[5]. A feature of the model was σ_a in Eq.(2), which expresses isotropic deformation resistance by the dynamic strain aging effect. The aging stress evolves nonlinearly with progress of the inelastic strain, as described by Eq.(4). The evolution rate of the aging stress depends on its evolutionary direction[6]. A recovering rate and a hardening rate of the aging stress were prescribed by Eq.(5) and Eq.(6), respectively. The negative rate dependency of the aging stress was expressed by Eq.(7) with a negative value of the material constant B.

3.3 Determination of material constants

As the proposed model has three stress components and many material constants, it was difficult to determine the material constants adequately by a usual procedure. Therefore, the authors tried to determine the material constants by measuring the each stress component experimentally.

1) Measuring of aging stress

Strain rate change tests were conducted with Mod.9Cr-1Mo steel to measure the aging stress. Figure 9 shows a stress-strain response of the tests schematically. When strain rate changes from fast to slow, the stress drops rapidly below corresponding constant slow tension curve. With progress of the inelastic strain, the stress gradually grows to the level of the slow constant rate tension curve. Based on the aging stress concept[6], the difference between the minimum stress just after strain rate change and the slow tension curve can be considered as the aging stress for the corresponding slow strain rate, because the stress just after the strain rate change consists of the backstress and the overstress and no aging stress exists.

Test material, test specimen, test facility and test temperatures were the same as those explained in section 2. The strain rate was changed only once at the point of tensile strain 1.0%. The strain rate of former loading was equal to $10^{-3}s^{-1}$ and that of latter loading was in the range of between $2x10^{-8}s^{-1}$ and $10^{-4}s^{-1}$.

Figure 10 shows the test results as relationships between the measured aging stress and the inelastic strain rate. The value of the measured aging stress increased with decrease of the inelastic strain rate. As for the temperature dependency, the aging stress showed higher value when the test temperature was low.

2) Measuring of backstress and overstress

Strain dip tests[7] were conducted to measure the backstress and the overstress. Figure 11 schematically shows an unloading curve of the tests by stress versus inelastic strain. The bowing-out behavior, which means that the inelastic deformation progresses during unloading was observed. Based on the overstress concept[7], the central point of the stress for maximum inelastic strain region can be considered as the backstress for the prior loading strain rate, because the overstress is equal to zero at the maximum inelastic strain region and radius of the elastic region was thought to be the aging stress. The overstress can be determined by subtracting the backstress and the above measured aging stress from the applied peak stress.

Test material, test specimen, test facility and test temperatures were the same as those described in section 2. The loading strain rate was in the range of between $10^{-6}s^{-1}$ and $10^{-3}s^{-1}$, and the unloading strain rate is equal to $10^{-3}s^{-1}$. The unloading was done at the point of 1.5%.

Figure 12 shows the test results as relationships between the backstress, the overstress and the inelastic strain rate. Value of the overstress depends not only on the strain rate but also on the test temperature, and it gets larger as the test temperature is higher. Value of the backstress depends on the test temperature too, and it gets smaller as the test temperature is higher. The backstress also shows the rate dependency owing to the static(thermal) recovery, and its degree gets larger as the test temperature is elevated.

3) Procedure of material constants determination

The material constants were systematically determined with each measured stress component, as follows.

A) The constants A and B in Eq.(7) were directly determined with the data of the aging stress in Fig.7.

B) Suppose that the backstress saturates at tensile strain 1.5%, the constant a in Eq.(3) was determined with the data of the backstress for $10^{-3}s^{-1}$ in Fig.9.

C) The constant C in Eq.(3) was determined to express the hardening behavior of the monotonic curve under fast loading condition($10^{-3}s^{-1}$).

D) The constants D and n in Eq.(2) were directly determined with the data of the overstress in Fig.9.

E) The constants γ and m in Eq.(3) were determined with the data of the backstress in Fig.9 basically.

F) The constant b_1 in Eq.(5) and the constant b_2 in Eq.(6) were determined to express the transient behavior under the strain rate change loading condition.

Table 4 shows values of the material constants thus determined.

3.4 Simulation

In order to evaluate the validity of the model, numerical simulations were done for various loading conditions.

Figures 3,4,13 and 14 show comparisons between the simulations and the experimental results at 550°C, where Mod.9Cr-1Mo steel shows large time/rate dependency. In Fig.3, the rate dependency of the monotonic curves was described with high accuracy. In Fig.4, the stress relaxation behavior was precisely predicted, including the dependency of the relaxed stress on prior loading strain rate. In Fig.13, creep curves[8] were also predicted very well. In Fig. 14, the stress-strain response under the strain rate change condition was accurately simulated, including the transient behavior.

Figures 5 and 6 show comparisons between the simulations and the experimental results at 400°C, where the steel shows the time dependency but no rate dependency. In Fig.5, the rate independent behavior of the monotonic curves was precisely described. In Fig.6, the stress relaxation behavior was expressed with high accuracy, while the monotonic curves show the rate independency.

At other temperatures(200°C, 500°C and 600°C), the simulations precisely agreed with the experimental results too.

4. CONCLUSION

In this study, inelastic behavior of Mod.9Cr-1Mo steel was investigated and a constitutive model considering dynamic strain aging effect was developed . Following conclusions were obtained.

1) Interesting behavior which was hardly described by conventional existing constitutive models was observed with Mod.9Cr-1Mo steel.
2) The unified constitutive model incorporating the dynamic strain aging effect was successful in describing the inelastic behavior of the steel precisely.

REFERENCES

1. Asada,Y., Ueta,M., Ichimiya,M., Douzaki,K., Nishida,T., Sakon,T., Mori,K. and Sukekawa,M. 1991. Research and Development on 9Cr-Steels for Steam Generator of DFBR in Japan(2) - Creep Properties - . *Proc. 11th SMiRT*, Vol.L, pp.115-120
2. Bodner,S.R. 1987. Review on a Unified Elastic-Viscoplastic Theory. *Unified Constitutive Equations for Creep and Plasticities*. Edited by A.K.Miller, Elsevier Applied Science, pp.273-302
3. Ruggles,M.B., Cheng,S. and Krempl,E. 1991. The Rate(Time)-Dependent Mechanical Behavior of Modified 9Cr-1Mo Steel (1) - Experiment at 538°C - . *Proc.11 SMiRT*, Vol.L, pp.145-150
4. Miller, A.K. and Sherby, O.D. 1978. A Simplified Phenomenological Model for Non-Elastic Deformation: Predictions of Pure Aluminum Behavior and Incorporation of Solute Strengthening Effects. *Acta Metallurgica*. Vol.26, pp.289-304
5. Chaboche,J.L. 1989. Constitutive Equations for Cyclic Plasticity and Cyclic Viscoplasticity. *International Journal of Plasticity*. Vol.5, pp.247-302
6. Oyamada,T. and Kaneko,K. 1994. Influence of Prestraining and Deformation Rate on Viscoplasticity and Strain Ageing of Metal Materials (2nd Report, The Case of Stress Relaxation of SCM435 Steel under Uniaxial Loading). *Trans.JSME*, Series A, Vol.60, pp.1397-

1401 (in Japanese)
7. Yaguchi,M., Okamoto,Y., Nakamura,T. and Asada,Y. 1995. Creep-Fatigue Interaction of Modified 9Cr-1Mo Steel in a Very High Vacuum Environment and Experimental Analysis of Overstress. *JSME International Journal*, Series-A, Vol.38 No.2, pp.220-225
8. Ruggles,M.B. and Ogata,T. 1994. Creep-Fatigue Criteria and Inelastic Behavior of Modified 9Cr-1Mo Steel at Elevated Temperature. *EPRI/CRIEPI Joint Studies*, Final Report

Table 1 Chemical composition of material (wt%)

C	Si	Mn	P	S	Ni	Cr	Mo	Nb	V	Al
0.09	0.24	0.44	0.003	0.001	0.04	8.78	0.94	0.08	0.21	0.013

Table 2 Mechanical properties at R.T.

Proof Stress (MPa)	Tensile Stress (MPa)	Elongation (%)	Reduction of Area (%)
528	630	26.0	70.0

Table 3 Material constants in Eq.(1)

Temperature	Strain Rate	M_1	M_2
473~733K	$10^{-6}\sim10^{-3}s^{-1}$	4.42×10^{2}	1.54×10^{2}
733~873K	$10^{-3}s^{-1}$	4.72×10^{1}	1.83×10^{3}
	$10^{-4}s^{-1}$	4.77×10^{1}	1.79×10^{3}
	$10^{-5}s^{-1}$	8.31	3.10×10^{3}
	$10^{-6}s^{-1}$	3.05	3.80×10^{3}

Note: Stress in MPa, Temp. in K

Table 4 Material constants of the constitutive model

Constants / Temperature	D	n	C	a	γ	m	b_1	b_2	A	B	E
200℃	738.9	2.66	1500.0	540.0	0	0	1000.0	500.0	-120.5	-32.1	200000.0
400℃	829.1	2.61	1500.0	500.0	1.07×10^{-34}	12.0	1000.0	320.0	-59.8	-19.9	190000.0
500℃	721.7	2.94	1500.0	441.0	7.59×10^{-19}	6.75	1000.0	250.0	-53.4	-17.8	175000.0
550℃	889.1	2.85	1500.0	380.0	7.05×10^{-18}	6.75	1000.0	200.0	-60.2	-17.3	165000.0
600℃	1166.2	2.77	1500.0	280.0	6.60×10^{-17}	6.75	1000.0	180.0	-64.7	-17.8	155000.0

Initial Value: $X(0)=0$ $\sigma_a(0)=0$ Note: Stress in MPa, Strain in mm/mm, Time in sec

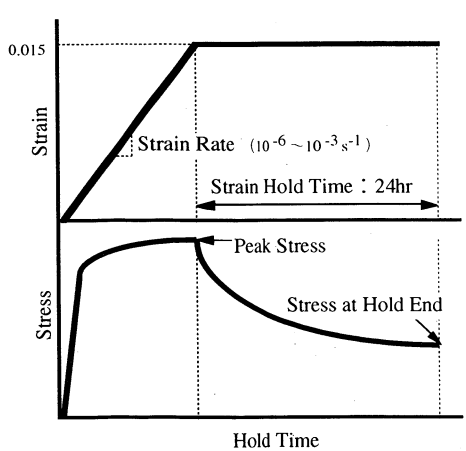

Fig.1 Loading conditions: monotonic tension and strain hold waveform

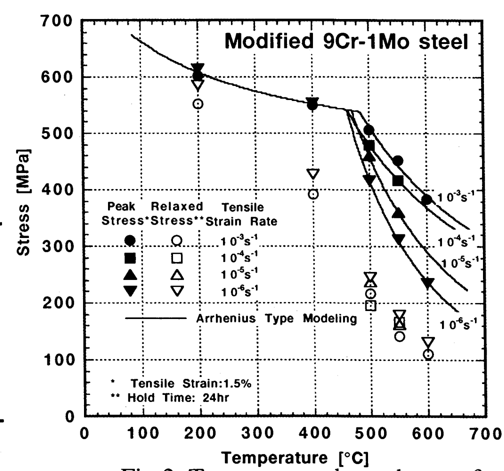

Fig.2 Temperature dependency of peak stress and relaxed stress

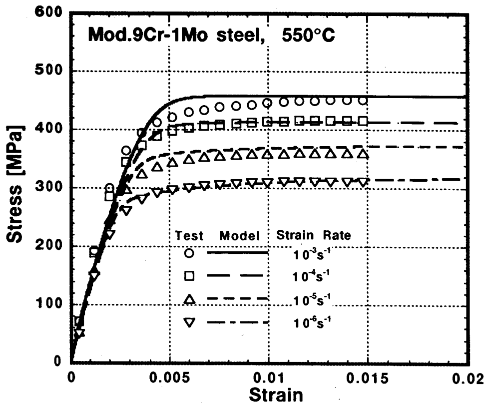

Fig.3 Test results and calculation results of monotonic behavior at 550°C

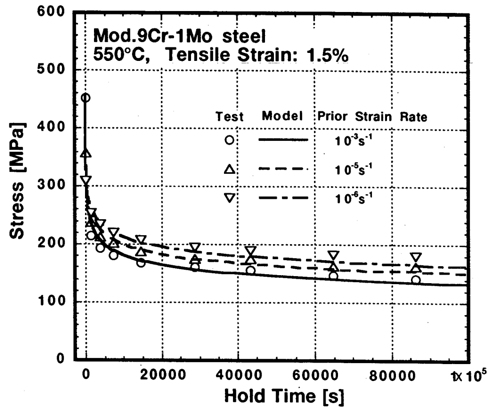

Fig.4 Test results and calculation results of relaxation behavior at 550°C

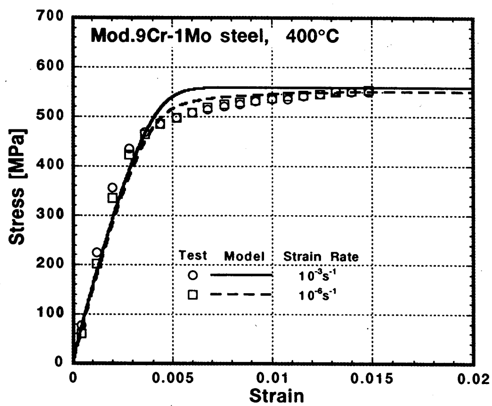

Fig.5 Test results and calculation results of monotonic behavior at 400°C

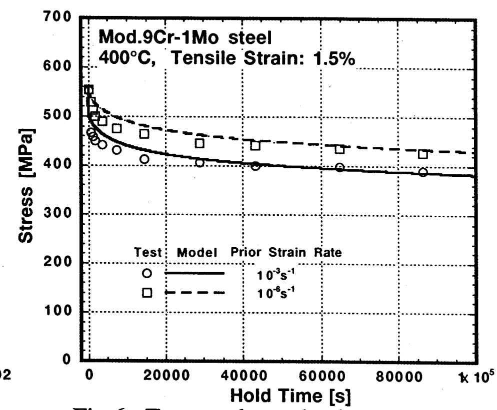

Fig.6 Test results and calculation results of relaxation behavior at 400°C

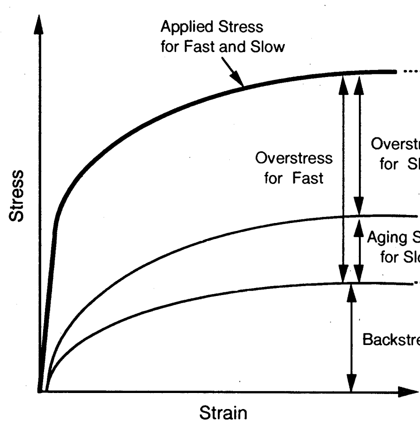

Fig.7 Schematic figure of the model for monotonic tension

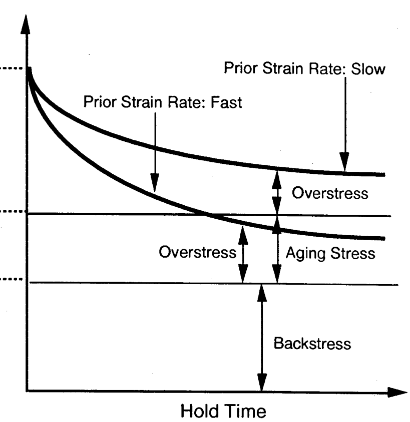

Fig.8 Schematic figure of the model for stress relaxation

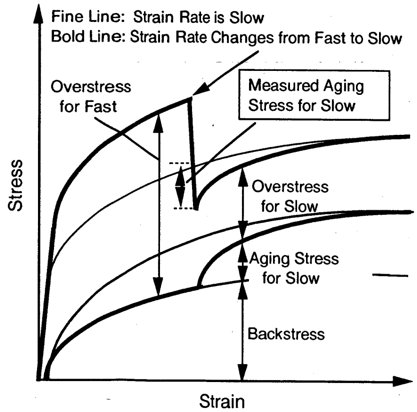

Fig.9 Schematic figure of determination of aging stress component

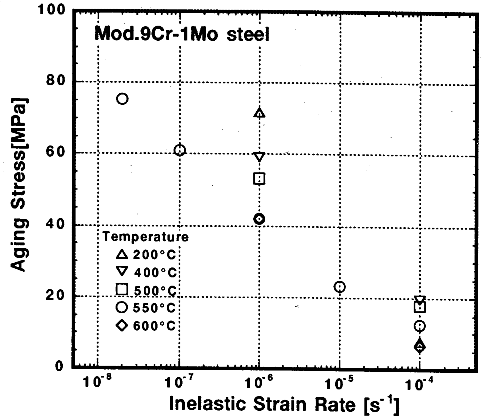

Fig.10 Relationship between measured aging stress and inelastic strain rate

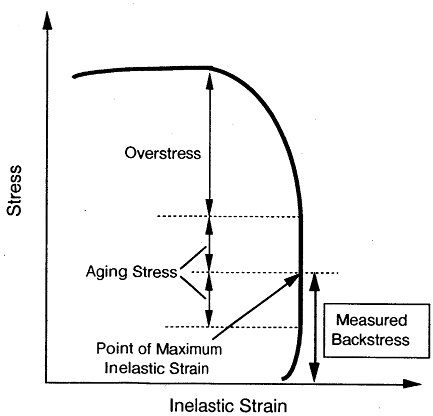

Fig.11 Schematic figure of determination of backstress and overstress

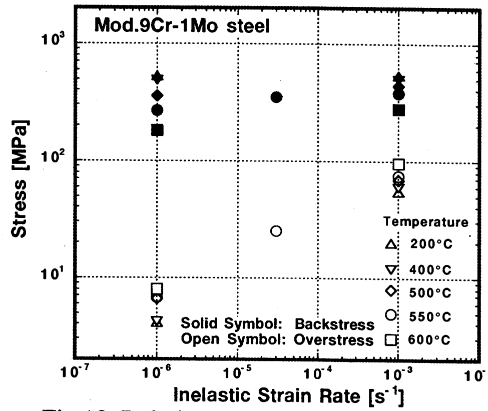

Fig.12 Relationship between measured back-stress, overstress and inelastic strain rate

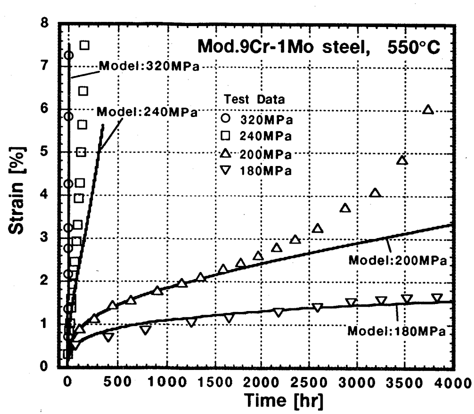

Fig.13 Test data[8] and calculation results of creep behavior at 550°C

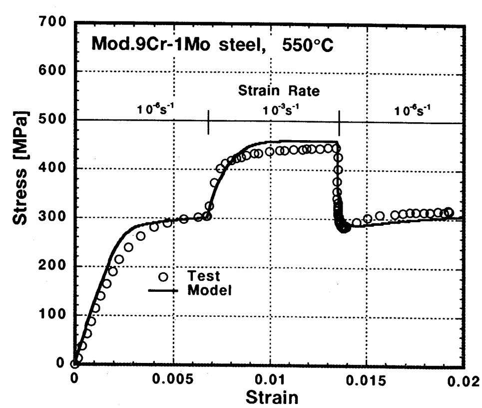

Fig.14 Test results and calculation results of strain rate change waveform at 550°C